Available online at www.sciencedirect.com
ScienceDirect
European Journal of Pharmaceutics and Biopharmaceutics 69 (2008) 496–507
European Journal of Pharmaceutics and Biopharmaceutics
www.elsevier.com/locate/ejpb

Research paper

An investigation into the relationship between carrier-based dry powder inhalation performance and formulation cohesive–adhesive force balances

Matthew D. Jones [a,1], Haggis Harris [a], Jennifer C. Hooton [a,2], Jagdeep Shur [a], Graeme S. King [a], Camilla A. Mathoulin [a], Katrina Nichol [a], Tracey L. Smith [a], Michelle L. Dawson [b], Alan R. Ferrie [b], Robert Price [a,*]

[a] *Department of Pharmacy and Pharmacology, University of Bath, Bath, UK*
[b] *GlaxoSmithKline Research and Development, Herts, UK*

Received 2 October 2007; accepted in revised form 28 November 2007
Available online 10 January 2008

Abstract

The inclusion of different carrier materials in a dry powder inhaler (DPI) system can alter formulation performance, which might be attributable to variation in the adhesion between drug and carrier particles. The aim of this study was, therefore, to further examine the relationship between drug-carrier adhesion and performance, by comparing data relating to many different drug-carrier combinations. Four drugs and four carriers were employed, giving a total of 16 combinations. The relative magnitude of the drug-carrier adhesion for each combination was quantified using the cohesion–adhesion balance (CAB) approach to colloidal probe atomic force microscopy. The *in vitro* inhalation performance of the 16 formulations (1.5% w/w drug) was investigated and found to vary significantly. Plots of fine particle dose against drug-carrier CAB ratio revealed that performance was optimised when the drug-carrier CAB ratio was slightly cohesive. This trend was found to fit with those from similar previous studies, although due to the smaller number of formulations investigated previously, the full extent of this relationship had not been revealed. It was concluded, therefore, that when developing a carrier-based DPI, the selection of a drug-carrier combination with a slightly cohesive CAB ratio might result in optimal performance.

Keywords: Adhesion; Agglomerate; Atomic force microscopy; Carrier; Cohesion; Dry powder inhaler

1. Introduction

The delivery of a drug to the lungs can only be achieved by a combination of inhaler device, drug formulation and inhalatory manoeuvre capable of producing an aerosol of drug particles with an aerodynamic diameter smaller than 5 μm [1,2]. This is often achieved in dry powder inhalers (DPIs) through the use of a micronised drug with a particle size smaller than 5 μm, which is dispersed during inhalation to ensure it reaches the patient's lungs [3]. Unfortunately, micronised powders are intrinsically cohesive and have poor flowability, leading to manufacturing problems, dose variability and poor aerosolisation [4]. The most common solution to the first two of these problems is to blend fine respirable drug particles with coarser particles of an inert excipient (usually α-lactose monohydrate), known as the carrier [4]. This results in a mixture with at least some of the fine drug particles adhered to the surface of the coarse carrier particles, and is known as a carrier-based DPI for-

* Corresponding author. Pharmaceutical Surface Science Research Group, Department of Pharmacy and Pharmacology, University of Bath, Bath BA2 7AY, UK. Tel.: +44 (0) 1225 383644; fax: +44 (0) 1225 386114.
E-mail address: R.Price@bath.ac.uk (R. Price).
[1] Present address: Department of Pharmaceutics, The School of Pharmacy, University of London, 29/39 Brunswick Square London, WC1N 1AX, UK.
[2] Present address: AstraZeneca R&D, Silk Road Business Park, Charter Way, Macclesfield, Cheshire SK10 2NA, UK.

0939-6411/$ - see front matter © 2007 Elsevier B.V. All rights reserved.
doi:10.1016/j.ejpb.2007.11.019

mulation. Such blends exhibit the necessary improvement in powder flow properties to enable metering and fluidization of the highly cohesive fine drug particles.

In order for the drug particles in a carrier-based DPI formulation to reach their site of action, they must detach from the surface of the carrier during the process of aerosolisation [4,5]. This is the key process that governs the performance of such formulations, and is dependent upon the balance between the cohesive and adhesive forces between drug and carrier particles and the aerodynamic drag forces acting to overcome them during aerosolisation [2,5].

It is, therefore, unsurprising that numerous studies have shown that changing the carrier material can influence fine particle delivery and, therefore, formulation performance, as such a change will also lead to different levels of drug-carrier adhesion [6]. Many different non-lactose carriers have been investigated, such as β-cyclodextrin, erythritol, glucose, maltitol, maltose, mannitol, raffinose pentahydrate, sorbitol, trehalose dihydrate and xylitol [7–19]. Differences in the performance of formulations containing different carrier materials have been attributed to differences in hygroscopicity [13,19], surface roughness [9,10], particle size or shape [15], surface energy [9,18] and drug-carrier adhesion [9,11].

DPI performance may also be altered by keeping the carrier material constant but changing its physicochemical properties. For example, whilst there have been conflicting results with regard to the effects of ''average'' carrier particle size (usually measured as volume equivalent diameter by laser diffraction) on drug delivery [6], it is widely acknowledged that carriers containing a higher proportion of fine particles produce greater formulation performance than carriers with a smaller proportion of fine particles [20]. Carrier particle shape is also known to affect performance, with more elongated particles of lactose being associated with increased drug delivery [21–23]. Formulation performance can also be affected by the surface roughness of carrier particles, but the relationship is complicated and appears to depend upon the scale of the roughness in relation to the size of the drug particles [6]. Finally, carrier flowability is known to effect the emission of drug from a DPI device and possibly the subsequent delivery of that drug to the lungs [6,24–26].

Despite the influence of the physicochemical properties of carrier particles on DPI performance, recent studies have suggested that the varying performance of formulations containing carriers of different materials could be attributed to differences in the relative drug-carrier adhesion, which could be measured by colloidal probe atomic force microscopy (AFM) [7,12]. This work utilised the recently developed cohesive–adhesive balance (CAB) approach, which can be used to measure the ratio between the cohesion of the drug with itself and its adhesion to the carrier [27]. A CAB ratio <1 indicates that, all other variables being equal, the drug is more adhesive to the carrier than cohesive with itself, and so might be expected to form a stable, ordered mixture upon blending [28]. A CAB ratio >1, however, indicates that the drug is more cohesive with itself than adhesive to the carrier, suggesting that upon blending a less uniform mixture might be produced, containing agglomerates of drug [28]. It was found that drug-carrier combinations with a higher CAB ratio resulted in a higher fine particle fraction (FPF) upon aerosolisation, despite potential difference between the carriers in terms of size, shape, roughness and flowability [7,12]. Such an approach might, therefore, represent a useful preformulation tool for the screening of potential formulation components during DPI development, but to date studies investigating this method have only employed a limited number of formulations with a limited range of drug-carrier CAB ratios [7,12]. In particular, only a limited number of drug-carrier combinations with a slightly adhesive (i.e. slightly <1) or slight cohesive (i.e. slightly >1) CAB ratio have been examined.

The CAB technique has also been employed to study the dispersion mechanisms of carrier-based DPI formulations containing different fine excipients [29]. The interactions of four drugs (budesonide, fluticasone propionate, formoterol fumarate dihydrate and salmeterol xinafoate) and four excipients (erythritol, α-lactose monohydrate, D-mannitol and α,α-trehalose dihydrate) were measured, giving a total of 16 CAB ratios, many of which fell in the slightly adhesive or cohesive region (Table 1). These ratios were measured between micronised drug particles and extremely smooth crystalline excipient surfaces using the standard CAB methodology employed originally by Begat et al. [27]. The aim of the work described here was, therefore, to further investigate the relationship between carrier-based formulation performance and drug-carrier CAB ratio, especially for formulations with a slightly adhesive or slightly cohesive CAB ratio. This was achieved by assessing the performance of the 16 binary (i.e. no added fines) formulations that could be produced using the four drugs and four excipients whose CAB ratios are listed in Table 1. Materials from the same batches as those used previously [29] were employed, to ensure that this comparison was valid. In addition, the four carriers were characterised using a number of techniques designed to assess their similarity in terms of the variables discussed above that are known to affect formulation performance, in order to validate (or otherwise) the comparison of formulations containing different carriers.

2. Materials and methods

2.1. Materials

Micronised fluticasone propionate (FP) and salmeterol xinafoate (SX) were donated by GlaxoSmithKline Research and Development (Ware, UK). Micronised budesonide and formoterol fumarate dihydrate (FFD) were supplied by Sicor (Santhia, Italy). Erythritol was donated by Cerestar (Castelmassa (Ro), Italy), D-mannitol was obtained from Sigma–Aldrich (Gillingham, UK), α-lactose monohydrate

Table 1
CAB ratios (± SD) for the interactions of drug colloidal probes with extremely smooth crystalline excipient substrates (data taken from Jones et al. [29], which used the same batches of material as this study)

CAB ratio ± SD	Colloidal probe			
	Micronised budesonide	Micronised FP	Micronised FFD	Micronised SX
Crystalline substrate				
Erythritol	0.96 ± 0.02	0.77 ± 0.05	1.00 ± 0.05	1.12 ± 0.02
Lactose	0.82 ± 0.08	0.22 ± 0.00	1.16 ± 0.11	2.39 ± 0.02
Mannitol	1.12 ± 0.06	0.46 ± 0.03	1.18 ± 0.07	0.65 ± 0.01
Trehalose	1.07 ± 0.06	0.70 ± 0.05	1.02 ± 0.10	1.37 ± 0.06

(*Lactohale*) was donated by Friesland Foods Domo-Pharma (Zwolle, The Netherlands) and α,α-trehalose dihydrate was donated by British Sugar (Peterborough, UK). From this point forward, these excipients will be referred to as erythritol, lactose, mannitol and trehalose. All solvents were supplied by Fisher Scientific UK (Loughborough, UK) and were of at least analytical grade. Water was purified by reverse osmosis (MilliQ, Molsheim, France).

2.2. Methods

2.2.1. Recrystallisation of carrier particles

As supplied, erythritol and trehalose had a coarse particle size to large for sieving into a 63–90 μm fraction. They were therefore recrystallised from solution to produce a more appropriate particle size range. Saturated solutions of each material in water were prepared, to which an anti-solvent (ethanol) was added at a rate of 20 ml min^{-1} until a water/ethanol mass ratio of 5:95 was reached. The resultant crystalline powder was collected by filtration and washed with ethanol. The erythritol powder was dried under a vacuum at 40 °C for 24 h. Given the ease with which trehalose dihydrate is known to dehydrate [30], the trehalose powder was left to air dry for 7 days.

2.2.2. X-ray powder diffraction

Erythritol and trehalose were analysed by X-ray powder diffraction (XRPD) to determine their crystallinity and polymorphism after recrystallisation. Diffractograms of each material before and after recrystallisation were obtained using a Phillips analytical X-ray powder diffractometer (Cambridge, UK) with a CuK_{α} source ($\lambda = 1.5418$ Å) operated at 40 kV and 25 mA. A single sweep between diffraction angles (2θ) 5° and 60° with a step size of 0.02° and step time of 1.3 s was employed for each measurement.

2.2.3. Sieving

The as received *Lactohale* (lactose) and mannitol, and the recrystallised erythritol and trehalose were sieved to produce 63–90 μm fraction carriers, using stainless steel sieves (Endecotts Limited, London, UK) and an Analysette 3 PRO vibratory sieve shaker (Fritsch GmbH, Idar–Oberstein, Germany) at an amplitude of 0.8 mm and frequency of 50 Hz.

2.2.4. Particle size analysis

Particle size analysis was carried out in the dry state. Powders were dispersed with compressed air at 3 bar (drugs) or 2 bar (carriers) through a RODOS dry disperser fed by an ASPIROS micro-dosing unit before sizing with a HELOS laser diffraction sensor (all from Sympatec GmbH, Clausthal–Zellerfeld, Germany). Dispersion pressures were chosen following pressure titration experiments, to ensure complete separation of particles without the breakage of whole particles. The particle size analysis was performed using WINDOX 4.0 software (Sympatec GmbH, Clausthal–Zellerfeld, Germany). Size distributions and summary statistics are the average of three determinations.

2.2.5. Scanning electron microscopy

Particle size and shape were qualitatively assessed using scanning electron microscopy (SEM). Samples were fixed to sticky carbon tabs mounted on aluminium stubs and excess powder removed with a puff of air. They were then coated with gold (~20 nm thickness) using a S150B sputter coater (Edwards High Vacuum, Sussex, UK) and examined using a scanning electron microscope (model JSM6310, Japanese Electron Optics Ltd., Tokyo, Japan) at 10 KeV.

2.2.6. Particle shape analysis

The particle shape of the sieved carriers was quantitatively assessed using dynamic image analysis. The powders were dispersed with compressed air at 2 bar through a RODOS dry disperser and fed into a QICPIC image analysis sensor (both from Sympatec GmbH, Clausthal–Zellerfeld, Germany). Images of at least 100,000 particles of each sample were captured and analysed, and the resultant data processed to calculate the aspect ratio and circularity of each particle, thus enabling the construction of particle shape distributions and summary statistics. The aspect ratio of each particle was defined as the ratio between its minimum and maximum Feret's diameters (i.e. aspect ratio = minimum Feret's diameter/maximum Feret's diameter). The circularity of each particle was defined as the ratio between the circumference of a circle with the same projected area as the particle and the actual circumference of the particle (i.e. circularity = circumference of equivalent area circle/actual circumference of particle). Both these parameters could, therefore, vary between 0 and 1, with 1

representing perfect sphericity and smaller values progressively more irregular particle shapes.

2.2.7. Atomic force microscopy

The surface topography of the 63–90 μm carriers was investigated with TappingMode™ atomic force microscopy (AFM) using a Multimode AFM, J-type scanner, Nanoscope IIIa controller (all from DI, Cambridge, UK) and a silicon tip (model number OMCL-AC240TS, Olympus, Japan) to image three randomly selected 10 μm × 10 μm square areas on the surface of particles of each material with a resolution of 512 × 512 pixels and a scan rate of 1 Hz. The roughness of imaged areas was quantified using the mean (R_a) and root mean square (R_q) of the variations in the height of the imaged surface, as calculated by the AFM software using the following equations [31]:

$$R_a = \frac{1}{n_p}\sum_{i=1}^{n}|y_i| \quad (1)$$

$$R_q = \sqrt{\frac{1}{n_p}\sum_{i=1}^{n}y_i^2} \quad (2)$$

where n_p is the number of points in the image and y_i is the distance of point i from the centre line.

2.2.8. Flowability

The flow properties of the 63–90 μm carriers were measured using a RST-XS annular ring shear tester controlled by RST-Control 95 software (both from Dietmar Schulze Schüttgutmesstechnik, Wolfenbüttel, Germany). Powders were stored at 25 ± 1 °C and 44% RH for 48 h prior to analysis, whilst analysis was carried out in an air conditioned laboratory maintained at 25 ± 1 °C and 35 ± 3% RH.

For each test, a 30 ml annular shear cell was filled with the material under investigation without applying force to the upper surface of the powder bed. This was presheared with a normal stress of 2500 Pa (σ_{pre}) until steady-state flow was achieved. A σ_{pre} value of 2500 Pa was chosen to reflect the consolidation stresses encountered by pharmaceutical powders during small scale powder handling and dosing operations [32], such as DPI manufacture. A yield locus was then constructed by measuring the shear stress required to cause the powder to fail under four normal stresses less than σ_{pre} (500 Pa, 1000 Pa, 1500 Pa and 2000 Pa) and the flowability calculated using the instrument software. Each powder was tested three times and the mean flowability ratio (ff_c) calculated. This is the ratio between the consolidation stress and unconfined yield strength of the powder (parameters which can be determined from the yield locus) and is a dimensionless parameter which increases as powder flowability improves [32].

2.2.9. In vitro formulation testing

2.2.9.1. Formulation blending. Each sieved carrier was blended in turn with each drug to produce 16 different binary DPI formulations. Four grams blends containing 1.5% w/w drug were prepared by geometrically mixing the drug and carrier lactose in a 15 ml glass tube for 60 s on a Whirlimixer (Fisons Scientific Equipment, Loughborough, UK). Each resultant blend was further mixed using a Turbula shaker–mixer (Willy A Bachofen AG, Basel, Switzerland) at 46 rpm for 40 min.

2.2.9.2. Content uniformity determination. Following blending, the drug content uniformity of all the formulations was assessed. Each formulation was spread evenly over a clean surface and ten samples of 33 ± 1 mg taken from random positions. Each sample was dissolved in a suitable solvent to 50 ml final volume and drug concentration assessed using high performance liquid chromatography (HPLC). The proportion of drug in each sample was calculated and the content uniformity expressed as the relative standard deviation (RSD).

2.2.9.3. Capsule filling. Each formulation was manually loaded into size 3 gelatin capsules (donated by Capsugel, Bornem, Belgium). Fill weight was 33 ± 1 mg, giving a nominal dose of 482 ± 15 μg drug per capsule. Following filling, capsules were stored in a sealed desiccator containing a saturated solution of potassium carbonate (giving a relative humidity of 44% [33]) for at least 24 h prior to analysis.

2.2.9.4. Formulation performance analysis. The performance of each formulation was assessed using an Andersen cascade impactor (ACI) with a pre-separator containing 10 ml water. Before use, the impaction plates were coated with silicone oil by immersion in a 1% solution in hexane and air drying. A *Rotahaler*® (GlaxoSmithKline, Ware, UK) was attached to the throat of the ACI (Copley Scientific Ltd., Nottingham, UK) using a rubber mouthpiece, a capsule inserted and then opened by twisting the inhaler body. The contents of the capsule were aerosolised into the ACI at a flow rate of 60 l min^{-1} for 4 s. Once the contents of ten capsules had been aerosolised, the inhaler and capsules, and each part of the ACI, were washed down into separate known volumes of a suitable solvent. The concentration of drug in each solution was determined by HPLC, from which the mass of drug deposited on each part of the ACI could be determined.

Each formulation was tested three times. To allow valid comparison of formulations with different recovered doses, the results were normalised to 100% drug recovery. This enabled the following parameters to be calculated: emitted dose per capsule (ED, mass of drug recovered from all parts of the ACI), fine particle dose per capsule (FPD, the mass of drug recovered from stages 1 and below of the ACI (<6.18 μm [34,35])) and FPF (the FPD expressed as a percentage of the ED). Analysis of variance (ANOVA) was used to compare mean results and where significant differences were found ($p < 0.05$), these were located with Tukey's Honestly Significant Difference (HSD) test.

3. Results and discussion

3.1. X-ray powder diffraction

Comparison of the XRPD patterns of the recrystallised carriers with those of the starting materials confirmed that the recrystallisation process resulted in crystalline erythritol (of which there is only one known polymorph) and trehalose dihydrate, as each pair of diffractograms showed peaks at the same diffraction angles. In addition, the diffraction patterns of trehalose dihydrate were comparable with previously published data for this material [30]. There were changes in the relative intensity of the diffraction peaks before and after recrystallisation, which can be attributed to variation in sample geometry and particle size.

3.2. Particle size analysis

The particle size distributions of the drugs each approximated to a log–normal distribution, and were therefore summarised using the d_{10}, d_{50} and d_{90} values and the proportion of particles smaller than 5 μm (see Table 2). These distributions and summary statistics were essentially similar, with the vast majority of particles smaller than 5 μm diameter, suggesting that the drug powders were suitable for DPI formulation [2]. However, it should be noted that laser diffraction measures geometric diameter, whereas particle deposition is determined by aerodynamic diameter, so a direct comparison between proportion of particles <5 μm diameter and FPD cannot necessarily be drawn.

The particle size distributions of the sieved carriers each approximately followed a negatively skewed log–normal distribution and so were summarised using the d_{10}, d_{50} and d_{90} values and the proportion of particles smaller than 10 μm diameter (see Table 2). Comparison of these particle size distributions and the summary statistics revealed that despite careful sieving into the same size fraction, the four carrier materials did not have identical particle size distributions. This is reflected by the results of statistical analysis using ANOVA, which found significant differences in the data for each of the carrier particle size descriptors shown in Table 2 ($p < 0.001$ in all cases). In particular, the particle size distributions differed towards smaller particle diameters (<50 μm), which is reflected by considerable differences in the d_{10} and % <10 μm values (Table 2).

3.3. Scanning electron microscopy

Inspection of SEM images of the four micronised drugs (Fig. 1) confirms the particle size data presented above, with the majority of particles <5 μm diameter. Inspection of SEM images of the four 63–90 μm sieved carrier materials (Fig. 2) also correlates with the particle size data. The materials appeared to have approximately the same average particle size, but with varying proportions of intrinsic fines. These were especially evident in the SEMs of the lactose carrier, which was also found to have the largest proportion of intrinsic fines by laser diffraction particle size analysis (Table 2).

The particle shape of the four carriers differed considerably and was related to their underlying crystal habits. Erythritol particles had an irregular but smooth and rounded morphology, whilst lactose particles displayed the tomahawk shape typical of α-lactose monohydrate [36], with a considerable number of irregularly shaped fine particles both adhered and unadhered to the larger particles. Mannitol particles were elongated, with some almost needle shaped. They appeared to have been formed by the granulation of smaller particles, producing a rough surface. Finally, the trehalose particles were irregularly shaped but tended to be slightly elongated. They possessed smooth surfaces and many appeared to have been formed by the fusion of smaller particles.

3.4. Particle shape analysis

The aspect ratio and circularity distributions of the four carriers (not shown) showed considerable differences between the materials in terms of particle shape. These differences are reflected in the shape factor 50th percentile values shown in Table 3. These quantitative particle shape data clearly corroborate the qualitative assessment of shape achieved using SEM. Mannitol was associated with the smallest shape factors of the four materials, indicating that it was the least spherical of the carriers, which reflects its elongated shape observed by SEM. The remaining car-

Table 2
Summary particle size statistics of the study materials ($n = 3$)

	d_{10} (μm ± SD)	d_{50} (μm ± SD)	d_{90} (μm ± SD)	% <5 μm (±SD)	% <10 μm (±SD)
Micronised budesonide	0.46 ± 0.02	1.44 ± 0.01	3.62 ± 0.03	97.6 ± 0.17	—
Micronised FP	0.51 ± 0.05	1.79 ± 0.13	3.95 ± 0.26	96.7 ± 1.45	—
Micronised FFD	0.64 ± 0.01	1.70 ± 0.00	3.30 ± 0.02	99.2 ± 0.04	—
Micronised SX	0.53 ± 0.01	1.52 ± 0.02	3.54 ± 0.02	97.8 ± 0.06	—
Erythritol carrier	14.50 ± 1.28	67.74 ± 1.48	112.33 ± 2.14	—	7.2 ± 0.7
Lactose carrier	9.98 ± 0.92	60.69 ± 1.55	119.14 ± 2.26	—	10.0 ± 0.9
Mannitol carrier	18.49 ± 0.71	71.17 ± 0.80	140.38 ± 0.49	—	5.0 ± 0.3
Trehalose carrier	26.22 ± 0.72	74.16 ± 1.12	118.65 ± 1.09	—	3.4 ± 0.1

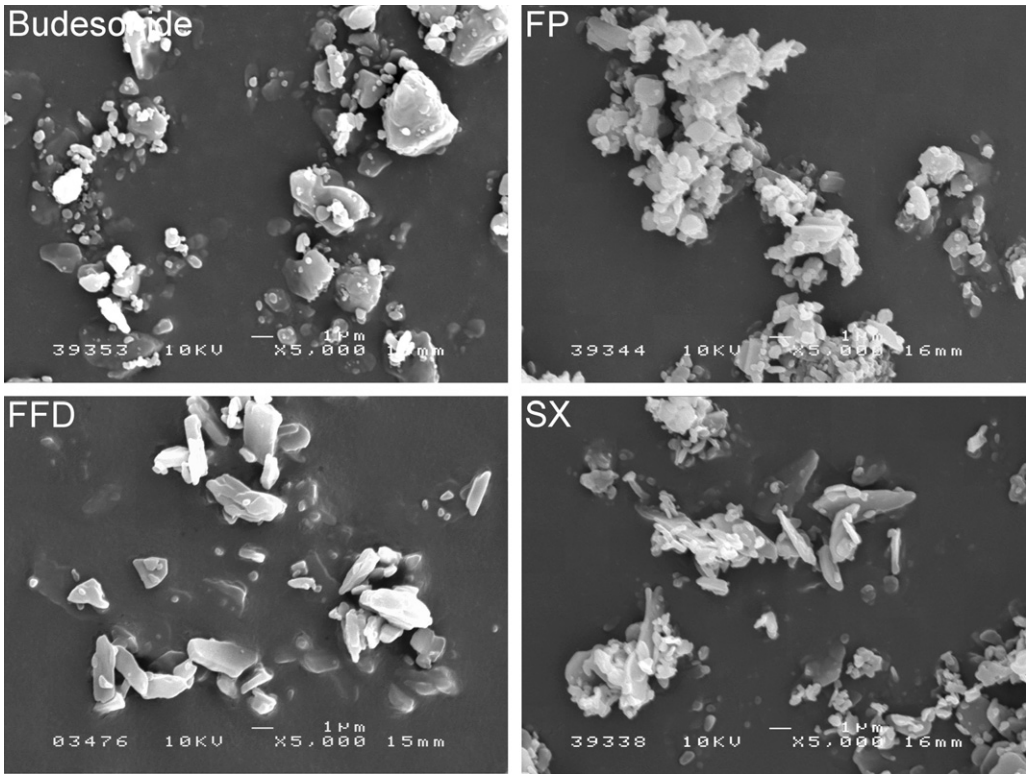

Fig. 1. Representative SEM images of the four micronised drugs.

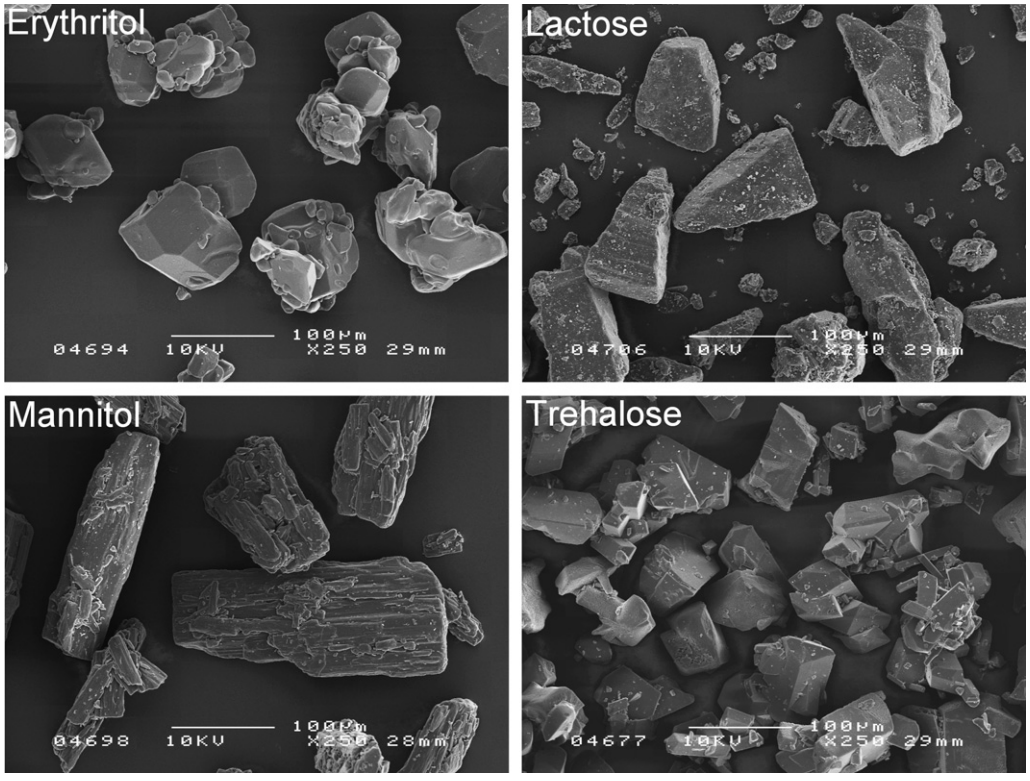

Fig. 2. Representative SEM images of the four 63–90 μm sieved carriers.

riers approached sphericity in the order lactose < trehalose < erythritol, which reflected the tomahawk, slightly elongated and rounded morphologies of these respective materials as observed by SEM.

Table 3
Particle shape, surface roughness and flowability data for the four 63–90 μm carriers

	Aspect ratio 50th percentile	Circularity 50th percentile	Mean R_a (nm ± SD)	Mean R_q (nm ± SD)	Mean flowability (ff_c ± SD)
Erythritol	0.75	0.89	16.46 ± 13.65	23.77 ± 20.09	6.10 ± 0.49
Lactose	0.64	0.87	52.09 ± 9.44	75.43 ± 13.89	4.79 ± 0.27
Mannitol	0.56	0.84	30.22 ± 9.55	49.25 ± 21.21	13.61 ± 0.35
Trehalose	0.71	0.88	85.20 ± 16.13	113.46 ± 22.11	13.01 ± 0.45

R_a = mean roughness (Eq. (1)); R_q = root-mean-square roughness (Eq. (2)).

3.5. Atomic force microscopy

TappingMode™ AFM was employed to quantify the nanoscale surface roughness of the carrier materials. Inspection of the AFM images (not shown) revealed qualitative differences between the roughness of the carriers, with erythritol appearing reasonably smooth, lactose and trehalose exhibiting an irregular pattern of rounded asperities and mannitol displaying a series of linear feature that might reflect its granulated appearance when observed by SEM. This qualitative impression was upheld by the differences in the roughness parameters (Table 3). ANOVA found significant differences in both the R_a ($p = 0.001$) and the R_q ($p = 0.003$), with subsequent analysis using Tukey's HSD test revealing that the trehalose carrier was significantly rougher than the other materials and that the lactose carrier was significantly rougher than the erythritol carrier.

3.6. Flowability

As Table 3 shows, the flowability of the four 63–90 μm sieved carriers showed considerable differences. These were found to be significant using ANOVA ($p < 0.001$), with significant flowability differences being located between all the carriers (apart from mannitol and trehalose) using Tukey's HSD test. As the carriers have already been shown to have different particle size distributions, particle shapes and surface roughness, which are all variables known to effect powder flow [35,37], it is unsurprising that they were found to have such markedly different flowability. In particular, it is evident from studying Tables 2 and 3 that lactose and erythritol had poorer flowability than mannitol and trehalose, which may be related to the greater fine excipient content of both lactose and erythritol.

3.7. In vitro formulation testing

3.7.1. Content uniformity

The RSD of the drug content of the 16 formulations tested is shown in Table 4. As these data show, not all the formulations had a drug RSD <6%, which is the value commonly taken as sufficiently uniform for DPI systems. As in previous work [7,29], however, for the purposes of this study it was important that all formulations were blended with a consistent method, in order to allow the effects of varying drug-carrier CAB ratios to be seen. In addition, a relatively low shear blending procedure was employed to ensure that subtle differences in blend structure caused by varying CAB ratios would not be overcome by putting a large amount of energy into the formulation during mixing. The blending process was therefore not altered in order to bring the RSD of all the formulations to <6%. There was no apparent relationship between content uniformity and drug-carrier CAB ratio.

Table 4
Content uniformity (RSD, %) of each drug-carrier blend

	Budesonide	FP	FFD	SX
Erythritol	1.50	2.99	3.79	1.41
Lactose	6.88	5.87	5.10	4.93
Mannitol	4.35	8.89	5.56	7.67
Trehalose	4.75	8.47	5.64	5.69

3.7.2. Drug impactor deposition

Log-probability plots (not shown) of the aerodynamic particle size distribution of drug deposited on the ACI stages from each formulation were linear ($R^2 > 0.945$), demonstrating that the use of a pre-separator and coating of the impaction plates prevented particle bounce and re-entrainment within the ACI [38]. The *in vitro* performance of the formulations tested is summarised in Fig. 3. As shown, there were a considerable number of significant differences between both the FPD and FPF of the various formulations ($p \leqslant 0.001$ in each case). Using these data, it was possible to draw up rank orders of formulation performance categorised by either the drug or carrier. The rank orders by carrier were as follows (pairs of formulations enclosed in brackets can be ranked in either order, depending on whether FPF or FPD is used):

Budesonide formulations: (Lactose > Trehalose) > Mannitol > Erythritol
FP formulations: Lactose > Mannitol > Trehalose > Erythritol
FFD formulations: Lactose > (Trehalose > Erythritol) > Mannitol
SX formulations: Lactose > Erythritol > Mannitol > Trehalose

Inspection of these rank orders reveals that the lactose carrier produced the best performance for each of the drugs studied. This may reflect the larger proportion of intrinsic

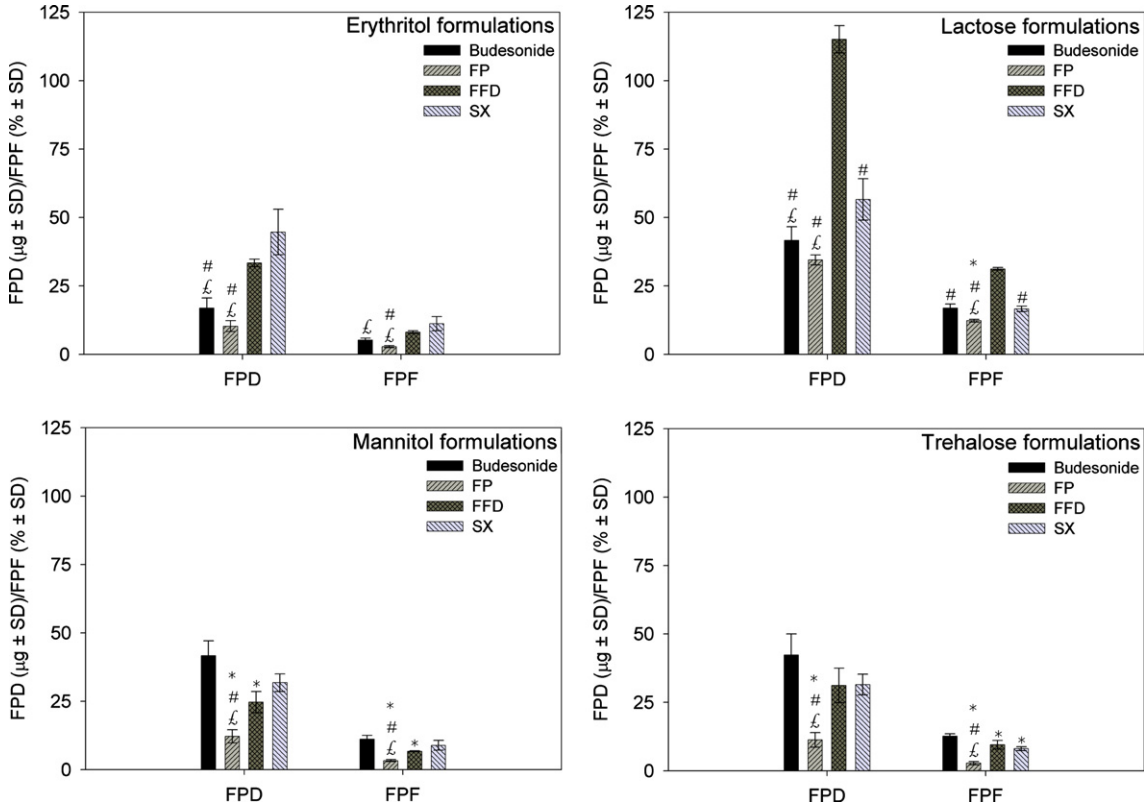

Fig. 3. FPD per capsule and FPF of the various drug-carrier combinations. *Significantly less than budesonide formulation; #significantly less than FFD formulation; £significantly less than SX formulation.

fines in this material (see Table 2), which is known to increase formulation performance [20]. The order in which the other carriers were ranked varied from drug-to-drug however, suggesting that the different levels of performance of these carriers are not attributable to one or more of their intrinsic properties, but to a property that changes depending upon the drug with which they are formulated. The magnitude of the drug-carrier adhesion is an example of such a property. The rank orders of performance by drug were as follows:

Erythritol formulations: SX > FFD > Budesonide > FP
Lactose formulations: FFD > (Budesonide > SX) > FP
Mannitol formulations: Budesonide > SX > FFD > FP
Trehalose formulations: Budesonide > (FFD > SX) > FP

Inspection of these ranks orders reveals that formulations of FP produced the poorest performance with each of the carriers studied. The order in which the other drugs were ranked varied from carrier-to-carrier, however. Once again, this suggests that the different levels of performance of these drugs are not attributable to one or more of their intrinsic properties, but to a property that changes depending upon the carrier with which they are formulated (for example, the magnitude of the drug-carrier adhesion). Given these findings, the aim of this study, which was the comparison of formulation performance with drug-carrier CAB ratios, appears valid, and is, therefore, considered in the following section.

3.8. The relationship between drug-carrier CAB ratio and formulation performance

As in previous work [7,12,29], comparison between formulation performance (FPD) and CAB ratio was made graphically. CAB ratios (Table 1) were obtained from the previous study (discussed above), which employed the same batches of drugs and excipients as this study [29]. In an attempt to negate the effects of the differing intrinsic properties of the carriers and drugs, the comparison with drug-carrier CAB ratio was made in two ways, categorised by either drug or carrier.

There was no consistent relationship between FPD and drug-carrier CAB ratio when the data were categorised by the drug (not shown). The performance data for budesonide and FFD showed no clear trends in relation to drug-carrier CAB ratio. FP and SX each appeared to show a weak trend, but the FPD of FP decreased with increasing drug-carrier CAB ratio, whilst the FPD of SX increased.

Given the large and significant differences between the carrier materials, in terms of particle size, shape, roughness and flowability, it is unsurprising that data relating to one drug formulated with four different carriers did not show any relationship between drug-carrier CAB ratio and formulation performance. As discussed above, these differ-

ences between the carriers are all known to affect DPI performance in complex and possibly interacting ways. Their effects on FPD can be presumed, therefore, to have been sufficiently large to mask any effects that changes in the drug-carrier CAB ratio may have had on formulation performance.

From the data presented above, it is apparent that the four drugs were more similar to each other than the carriers were similar to each other. This is unsurprising, as the drugs had been micronised, which is a sufficiently energetic process to have overcome differences in size and shape caused by the different drugs having different crystal habits. The result is that the micronised drugs were, in terms of their physical characteristics, reasonably similar to each other. On the other hand, the carrier materials had not been subjected to energetic post-crystallisation processing, meaning that differences in their size and shape caused by their different crystal habits had not been overcome.

Given that, in terms of their physical characteristics, the drugs were more similar to each other than the carriers were similar to each other, the comparison between formulation FPD and drug-carrier CAB ratio was repeated, with the data categorised by the carrier (Fig. 4). As Fig. 4 shows, this was successful in revealing a consistent relationship between the two variables. Although the absolute FPD associated with a particular drug-carrier CAB ratio varied between the different carriers (which can be attributed to the varying intrinsic properties of these materials), the same relative trend in the relationship between performance and drug-carrier CAB ratio was observed in all cases. For each carrier, FPD was optimised when the drug-carrier CAB ratio was slightly cohesive: the optimum CAB ratio for the erythritol, lactose, mannitol and trehalose carriers was 1.12, 1.16, 1.12 and 1.07, respectively. Formulation performance became progressively poorer as the drug-carrier CAB ratio became more adhesive or cohesive.

Fig. 5 shows the relationship between binary formulation performance and drug-carrier CAB ratio found in two previous studies, which examined salbutamol sulphate [7] and budesonide [12] formulated with five different carriers. Performance is represented by FPF, as FPD was not reported. The study which examined budesonide measured drug-carrier CAB ratios using both the {002} and {102} faces of the budesonide crystal for the cohesive measurement [12], so both these sets of data are shown. It should be noted that these studies used a different drug concentration (0.61% w/w) and inhaler device (the *Cyclohaler*®) compared with this study [7,12].

Inspection of Fig. 5 reveals that the findings of both this study and the previous studies of salbutamol sulphate and budesonide (CAB ratio measured using the {002} budeso-

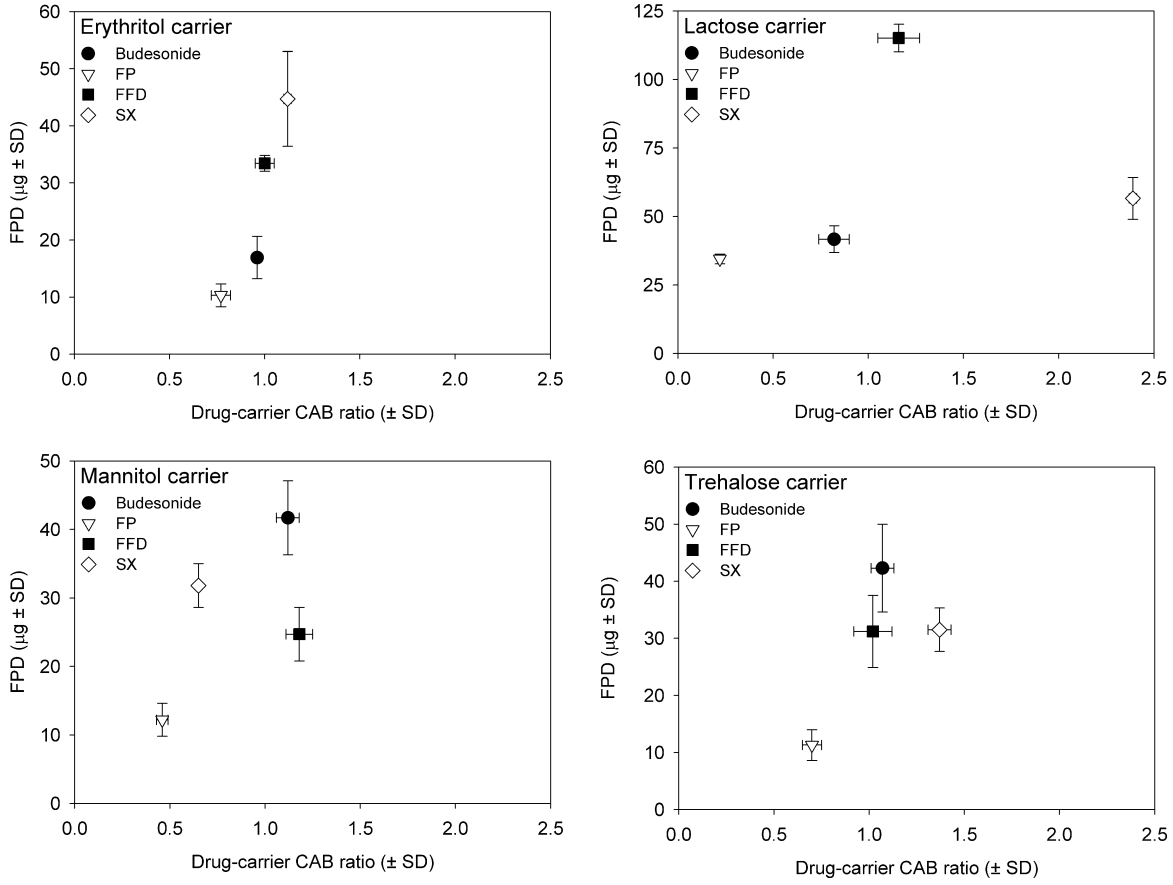

Fig. 4. The relationship between FPD and drug-carrier CAB ratio, categorised by carrier.

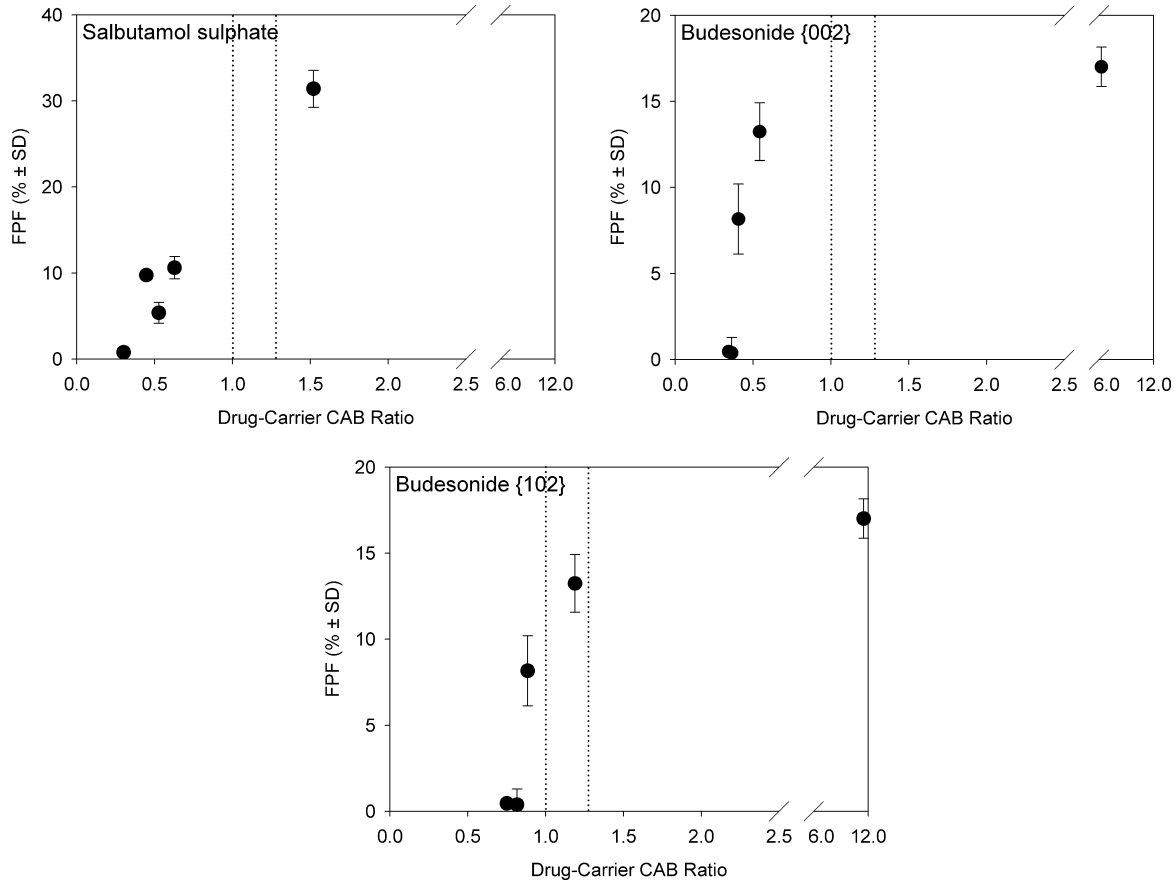

Fig. 5. The relationship between formulation FPF and drug-carrier CAB ratio found in previous studies of salbutamol sulphate [7] and budesonide (CAB ratios obtained using both the {002} and {102} faces of the budesonide crystal) [12]. The vertical dotted lines indicate the slightly cohesive drug-carrier CAB ratios that resulted in maximal formulation performance for the formulations described in this study.

nide crystal face) are in accordance with each other. These previous studies did not include formulations with a slightly cohesive drug-carrier CAB ratio and so did not show maximal performance in this area. Extrapolation of the available data suggests, however, that had these studies included a drug-carrier combination with a slightly cohesive CAB ratio, it might have produced the best performance. The data relating to budesonide produced using the {102} crystal face to measure the CAB ratio do not fit as well with the data from this study. This may be related to the inclusion of a formulation with an extremely cohesive drug-carrier CAB ratio (11.42), which may have behaved very differently to less cohesive formulations.

3.9. Interpreting the relationship between drug-carrier CAB ratio and formulation performance

The results of this study suggest that carrier-based DPI formulation performance is optimised when the drug-carrier CAB ratio is slightly cohesive. There are at least two explanations for these findings. Firstly, a more cohesive drug-carrier CAB ratio represents relatively weaker drug-carrier adhesion. If this were a reflection of weaker absolute drug-carrier adhesion, the greater performance seen with more cohesive drug-carrier CAB ratios could be attributed to the decreased force required to detach a drug particle from the carrier, resulting in the aerosolisation of a greater number of respirable drug particles. Secondly, the formation of larger drug-only agglomerates when the drug-carrier CAB ratio was more cohesive (as would be expected with a relatively more cohesive drug [28]) might also have resulted in improved formulation performance via an agglomeration mechanism recently proposed for other types of DPI formulation [28,29]. This proposes that larger agglomerates of particles are subject to greater deagglomeration forces in an airstream, as these forces are proportional to the square (drag force) or cube (collisions) of the diameter of the agglomerate. Larger agglomerates might therefore give rise to greater performance, as they might be more extensively broken down during aerosolisation and dispersion of the formulation. It is also possible that these two mechanisms might act alongside each other.

The first of these proposed mechanisms cannot explain why binary formulation performance decreased when the drug-carrier CAB ratio increased above the slightly cohesive region, as this represents a continued decrease in relative drug-carrier adhesion, which might have been expected to yield further increases in performance. However, under

the agglomeration mechanism, high drug-carrier CAB ratios represent relatively stronger drug cohesion. This might result in the formation of extremely strong drug-only agglomerates that resist extensive deagglomeration, giving poorer formulation performance.

4. Conclusions

The performance of the carrier-based DPI formulations employed in this study was optimised when a slightly cohesive drug-carrier CAB ratio was achieved. It can be concluded, therefore, that when developing a new formulation, the selection of a drug-carrier combination with a slightly cohesive drug-carrier CAB ratio might lead to optimum formulation performance. This finding might be explained by the agglomeration mechanism recently outlined for other types of DPI formulation [28,29]. In addition to being interesting in its own right, the applicability of this hypothesis to another type of formulation lends it further support. Further research is required to investigate whether these findings are applicable to formulations prepared using different techniques (especially higher shear blending) and aerosolised under different conditions.

Acknowledgements

The authors gratefully acknowledge the Engineering and Physical Sciences Research Council and GlaxoSmithKline for their generous funding of this work. The authors gratefully acknowledge the assistance of Barry Chapman (Department of Physics, University of Bath) in obtaining the XRPD data, Andy Smith (Sympatec Ltd.) in obtaining the particle shape data and Paul Vanden Branden (Scientific and Medical Products Ltd.) in obtaining the flowability data.

References

[1] D. Ganderton, The generation of respirable clouds from coarse powder aggregates, Journal of Biopharmaceutical Sciences 3 (1992) 101–105.
[2] H.W. Frijlink, A.H. de Boer, Dry powder inhalers for pulmonary drug delivery, Expert Opinion on Drug Delivery 1 (2004) 67–86.
[3] M.P. Timsina, G.P. Martin, C. Marriott, D. Ganderton, M. Yianneskis, Drug delivery to the respiratory tract using dry powder inhalers, International Journal of Pharmaceutics 101 (1994) 1–13.
[4] R.J. Malcolmson, J.K. Embleton, Dry powder formulations for pulmonary delivery, Pharmaceutical Science and Technology Today 1 (1998) 394–398.
[5] D. Ganderton, N.M. Kassem, Dry powder inhalers, in: D. Ganderton, T. Jones (Eds.), Advances in Pharmaceutical Sciences, Academic Press, London, UK, 1992, pp. 165–191.
[6] H.D.C. Smyth, A.J. Hickey, Carriers in drug powder delivery: implications for inhalation system design, American Journal of Drug Delivery 3 (2005) 117–132.
[7] J.C. Hooton, M.D. Jones, R. Price, Predicting the behaviour of novel sugar carriers for dry powder inhaler formulations via the use of a cohesive-adhesive force balance approach, Journal of Pharmaceutical Sciences 95 (2006) 1288–1297.
[8] X.M. Zeng, H.B. MacRitchie, C. Marriott, G.P. Martin, Humidity-induced changes of the aerodynamic properties of dry powder aerosol formulations containing different carriers, International Journal of Pharmaceutics 333 (2007) 45–55.
[9] G. Saint-Lorant, P. Leterme, A. Gayot, M.P. Flament, Influence of carrier on the performance of dry powder inhalers, International Journal of Pharmaceutics 334 (2007) 85–91.
[10] K. Endo, S. Amikawa, A. Matsumoto, N. Sahashi, S. Onoue, Erythritol-based dry powder of glucagon for pulmonary administration, International Journal of Pharmaceutics 290 (2005) 63–71.
[11] D. Traini, P.M. Young, M.D. Jones, S. Edge, R. Price, Comparative study of erythritol and lactose monohydrate as carriers for inhalation: atomic force microscopy and *in vitro* correlation, European Journal of Pharmaceutical Sciences 27 (2006) 243–251.
[12] J.C. Hooton, M.D. Jones, R. Price, The effect of the use of a cohesive drug when predicting performance of dry powder inhalation formulations through the cohesive adhesive balance technique, in: Proceedings of Drug Delivery to the Lungs 16, Edinburgh, UK, 2005, pp. 143–146.
[13] H. Steckel, N. Bolzen, Alternative sugars as potential carriers for dry powder inhalations, International Journal of Pharmaceutics 270 (2004) 297–306.
[14] D.L. French, D.A. Edwards, R.W. Niven, The influence of formulation on emission, deaggregation and deposition of dry powders for inhalation, Journal of Aerosol Science 27 (1996) 769–783.
[15] S.K. Tee, C. Marriott, X.M. Zeng, G.P. Martin, The use of different sugars as fine and coarse carriers for aerosolised salbutamol sulphate, International Journal of Pharmaceutics 208 (2000) 111–123.
[16] M.A. Braun, R. Oschmann, P.C. Schmidt, Influence of excipients and storage humidity on the deposition of disodium cromoglycate (DSCG) in the Twin Impinger, International Journal of Pharmaceutics 135 (1996) 53–62.
[17] P.R. Byron, V. Naini, E.M. Phillips, Drug carrier selection – important physicochemical characteristics, in: Proceedings of Respiratory Drug Delivery V, Phoenix, AZ, USA, 1996, pp. 103–114.
[18] D. Cline, R. Dalby, Predicting the quality of powders for inhalation from surface energy and area, Pharmaceutical Research 19 (2002) 1274–1277.
[19] P. Harjunen, T. Lankinen, H. Salonen, V.-P. Lehto, K. Jarvinen, Effects of carriers and storage of formulation on the lung deposition of a hydrophobic and hydrophilic drug from a DPI, International Journal of Pharmaceutics 263 (2003) 151–163.
[20] M.D. Jones, R. Price, The influence of fine excipient particles on the performance of carrier-based dry powder inhalation formulations, Pharmaceutical Research 23 (2006) 1665–1674.
[21] H. Larhrib, G.P. Martin, C. Marriott, D. Prime, The influence of carrier and drug morphology on drug delivery from dry powder formulations, International Journal of Pharmaceutics 257 (2003) 283–296.
[22] X.M. Zeng, G.P. Martin, C. Marriott, J. Pritchard, The influence of carrier morphology on drug delivery by dry powder inhalers, International Journal of Pharmaceutics 200 (2000) 93–106.
[23] F. Podczeck, The relationship between physical properties of lactose monohydrate and the aerodynamic behaviour of adhered drug particles, International Journal of Pharmaceutics 160 (1998) 119–130.
[24] R.G. Jiang, W.S. Pan, C.L. Wang, H. Liu, Use of recrystallized lactose as carrier for inhalation powder of interferon α2b, Pharmazie 60 (2005) 632–633.
[25] H. Murakoshi, T. Saotome, Y. Fujii, T. Ozeki, Y. Takashima, H. Yuasa, H. Okada, Effect of physical properties of carrier particles on drug emission from a dry powder inhaler device, Journal of Drug Delivery Science and Technology 15 (2005) 223–226.
[26] T. Nakate, H. Yoshida, A. Ohike, Y. Tokunaga, R. Ibuki, Y. Kawashima, Formulation development of inhalation powders for FK888 with carrier lactose using Spinhaler and its absorption in healthy volunteers, Journal of Controlled Release 97 (2004) 19–29.
[27] P. Begat, D.A.V. Morton, J.N. Staniforth, R. Price, The cohesive-adhesive balances in dry powder inhaler formulations I: direct quantification by atomic force microscopy, Pharmaceutical Research 21 (2004) 1591–1597.

[28] P. Begat, D.A.V. Morton, J.N. Staniforth, R. Price, The cohesive-adhesive balances in dry powder inhaler formulations II: influence on fine particle delivery characteristics, Pharmaceutical Research 21 (2004) 1826–1833.
[29] M.D. Jones, J.C. Hooton, M.L. Dawson, A.R. Ferrie, R. Price, An investigation into the dispersion mechanisms of ternary dry powder inhaler formulations by the quantification of interparticulate forces, Pharmaceutical Research, in press doi:10.1007/s11095-007-9467-1.
[30] M.D. Jones, J.C. Hooton, M.L. Dawson, A.R. Ferrie, R. Price, Dehydration of trehalose dihydrate at low relative humidity and ambient temperature, International Journal of Pharmaceutics 313 (2006) 87–98.
[31] F. Podczeck, Particle-particle adhesion in pharmaceutical powder handling, Imperial College Press, London, 1998.
[32] D. Schulze, Flow properties testing with ring shear testers RST-01.01, RST-01.pc and RST-XS, 2005.
[33] F.E.M. O'Brien, The control of humidity by saturated salt solutions, Journal of Scientific Instruments 25 (1948) 73–76.
[34] T. Srichana, P. Brain, C. Marriott, G.P. Martin, A study of drug-carrier interactions in dry powder inhaler formulations using the Andersen cascade impactor, X-ray microanalysis and time of flight aerosol beam spectrometry (TOFABS), Chemical and Pharmaceutical Bulletin 48 (2000) 167–174.
[35] X.M. Zeng, G.P. Martin, C. Marriott, Particulate interactions in dry powder formulations for inhalation, Taylor and Francis, London, 2001.
[36] S.L. Raghavan, R.I. Ristic, D.B. Sheen, J.N. Sherwood, L. Trowbridge, P. York, Morphology of crystals of α-lactose hydrate grown from aqueous solution, Journal of Physical Chemistry B 104 (2000) 12256–12262.
[37] D. Schulze, The behaviour of powders and bulk solids, Wolfenbüttel, Germany: Dietmar Schulze Schüttgutmesstechnik, 2004, http://www.dietmar-schulze.com/fre.html, date accessed: 10th January 2006.
[38] M. Hindle, P.R. Byron, N.C. Miller, Cascade impaction methods for dry powder inhalers using the high flowrate Marple-Miller Impactor, International Journal of Pharmaceutics 134 (1996) 137–146.